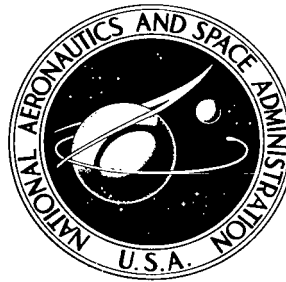


NASA TECHNICAL NOTE



NASA TN D-5629

C. 1

NASA TN D-5629



LOAN COPY: RETURN TO
AFWL (WL0L)
KIRTLAND AFB, N MEX

PHOSPHORUS DIFFUSION CONDITIONS FOR SHALLOW-JUNCTION SOLAR CELLS

by Harold E. Kautz
Lewis Research Center
Cleveland, Ohio



0132379

1. Report No. NASA TN D-5629	2. Government Accession No.	3. Recipient's Catalog No.	
4. Title and Subtitle PHOSPHORUS DIFFUSION CONDITIONS FOR SHALLOW-JUNCTION SOLAR CELLS		5. Report Date January 1970	
		6. Performing Organization Code	
7. Author(s) Harold E. Kautz	8. Performing Organization Report No. E-5341		
9. Performing Organization Name and Address Lewis Research Center National Aeronautics and Space Administration Cleveland, Ohio 44135	10. Work Unit No. 120-33		
	11. Contract or Grant No.		
	13. Type of Report and Period Covered Technical Note		
12. Sponsoring Agency Name and Address National Aeronautics and Space Administration Washington, D.C. 20546	14. Sponsoring Agency Code		
	15. Supplementary Notes		
16. Abstract Response to 0.4- μ m light and fill factor of shallow-junction n-on-p silicon solar cells was measured. Diffusion time, temperature, phosphorus source, and carrier gas were varied. The 0.4- μ m response increased with decreasing junction depth measured in terms of sheet conductance. For a sheet conductance less than 5×10^{-3} square/ohm, 0.4- μ m response and fill factor degraded with increased reverse leakage. The sources P_2O_5 and $POCl_3$ yielded more reproducible results than did elemental phosphorus. The P_2O_5 results were superior to $POCl_3$ results at 800° C but were equivalent up to 1000° C. Oxygen, nitrogen, and forming gas carriers yielded essentially equivalent results with constant sheet conductance.			
17. Key Words (Suggested by Author(s)) Solar cell Phosphorus diffusion		18. Distribution Statement Unclassified - unlimited	
19. Security Classif. (of this report) Unclassified	20. Security Classif. (of this page) Unclassified	21. No. of Pages 24	22. Price* \$3.00

*For sale by the Clearinghouse for Federal Scientific and Technical Information
Springfield, Virginia 22151

PHOSPHORUS DIFFUSION CONDITIONS FOR SHALLOW-JUNCTION SOLAR CELLS

by Harold E. Kautz

Lewis Research Center

SUMMARY

Phosphorus diffusion conditions for the fabrication of shallow-junction n-on-p silicon solar cells were studied. Variables examined included the time and temperature of diffusion as well as the phosphorus source material and carrier gas employed in the open-tube diffusion method. Sheet conductance on diffused wafers, as well as fill factor, reverse diode leakage, and short-circuit current response to 0.4-micrometer radiation of fabricated solar cells were measured. The 0.4-micrometer current response increased with conditions for decreasing junction depth, as evidenced by sheet conductance for all diffusion temperatures in the range 800° to 1000° C. However, for a sheet conductance less than about 5×10^{-3} square/ohm, both 0.4-micrometer response and fill factor were degraded because of increasing reverse diode leakage. The phosphorus sources phosphorus pentoxide (P_2O_5) and phosphorus oxychloride ($POCl_3$) yielded more reproducible results than those of elemental phosphorus in terms of sheet conductance. Phosphorus sources P_2O_5 and $POCl_3$ produced solar cells of essentially the same characteristics for diffusion temperatures above 800° C. At 800° C, the 0.4-micrometer response and fill factor of $POCl_3$ cells were somewhat lower than those of P_2O_5 cells.

Cells fabricated from diffusions employing oxygen as the carrier gas had lower sheet conductance than those fabricated with nitrogen or forming gas (6 percent hydrogen, 94 percent nitrogen) when all other variables were held constant. The 0.4-micrometer response of cells was independent of the carrier gas employed as measured at a constant sheet conductance.

INTRODUCTION

Present day silicon solar cells are fabricated with a phosphorus-diffused n-type layer on a p-type (usually 10 ohm-cm); boron-doped, single-crystal base material.

This n-on-p solar cell is a more favorable design in terms of radiation damage stability than the p-on-n alternative (refs. 1 and 2).

One approach to optimizing silicon solar cell efficiency is to maximize the current collected due to light actually absorbed in the cell. This current collection efficiency is affected by various diffusion conditions associated with producing the p-n junction within the cell. When the conditions are varied to produce shallower junctions, the solar cell response to the blue end of the visible spectrum is enhanced (ref. 3). As a result, the solar cells have greater stability to radiation damage. The blue wavelength range of light is absorbed very close to the illuminated surface. For example, over 95 percent of the 0.4-micrometer light is absorbed within 3 micrometers of the surface. Since the most extreme radiation damage experienced by cells in outer space degrades minority carrier diffusion length to a value not less than 10 micrometers, the blue light generated current collected from the n-region is essentially unaffected by radiation damage.

If the diffused junction is too shallow, however, one can expect to obtain high reverse leakage. This leakage results from poor junction formation and leads to degraded current output. Shallow junctions can also lead to low values of n-layer sheet conductance, which may cause excessive resistive losses.

These considerations imply the existence of optimum conditions in the diffusion process employed in forming the junction. The optimum condition may, however, vary with the application for which the cells are intended. High radiation environments would require the stability of high blue wavelength responses. In an environment where radiation is not a problem, the designer may wish to sacrifice blue wavelength response if other cell characteristics are thereby made more favorable.

On the basis of these considerations, it appears worthwhile to study more closely the dependence of solar cell characteristics on diffusion conditions.

In the present study, the conditions investigated were those associated with the open-tube method of diffusing phosphorus into silicon. They include the time, temperature, phosphorus source, and carrier gas employed to carry the phosphorus to the surface of the silicon slices. The effect of these parameters is measured in terms of the photovoltaic response of completed silicon solar cells. In all cases, the diffusion conditions are intended to produce saturated concentrations of phosphorus at the silicon surface.

THEORY

Spectral Response

The generation of excess minority carriers in a solar cell exposed to monochro-

matic light depends on the intensity of the light absorbed in the cell. The flux of photons R a distance X into the cell is

$$R = R_0 e^{-\alpha X} \quad (1)$$

where α is the absorption coefficient at the given wavelength. The rate of absorption is

$$\frac{-dR}{dX} = \alpha R_0 e^{-\alpha X} \quad (2)$$

If the junction depth is X_j and the distance to the back of the cell is X_B , the total light absorbed in the cell R_T is

$$R_T = \int_0^{X_j} \frac{dR}{dX} dX + \int_{X_j}^{X_B} \frac{dR}{dX} dX \quad (3)$$

Therefore,

$$R_T = R_0 \left(1 - e^{-\alpha X_j} \right) + R_0 \left(e^{-\alpha X_j} - e^{-\alpha X_B} \right) \quad (4)$$

The first term represents absorption in the diffused layer, and the second term represents absorption in the bulk region. Present day silicon solar cells have dimensions such that

$$X_B \approx 10^{-1} \text{ cm}$$

$$X_j < 10^{-4} \text{ cm}$$

For long wavelength radiation (red light), the absorption coefficient is (ref. 4)

$$\alpha \approx 10^2 \text{ cm}^{-1}$$

This implies that

$$e^{-\alpha X_j} \approx 1$$

Therefore, the long wavelength light absorption is entirely in the bulk region, and its magnitude will be independent of the junction depth.

For short wavelength radiation (blue light), the absorption coefficient is (ref. 4)

$$\alpha \approx 10^4 \text{ cm}^{-1}$$

and

$$e^{-\alpha X_B} \approx 0$$

Equation (4) for blue light then reduces to

$$R_T = R_0 \left(1 - e^{-\alpha X_j} \right) + R_0 e^{-\alpha X_j} \quad (5)$$

If the quantum efficiency is assumed to be 1, the rate of minority carrier generation will equal the rate of photon absorption of equation (5). The current I_α generated by the short wavelength radiation is thus

$$I_\alpha = I_D \left(1 - e^{-\alpha X_j} \right) + I_B e^{-\alpha X_j} \quad (6)$$

The short-circuit current produced by a solar cell depends on the rate of generation of minority carriers and the collection efficiency of the two regions of the cell. The collection efficiency of the two regions depends on the minority carrier lifetimes. Lifetimes in the bulk region are assumed to be so long that no significant recombination occurs in comparison to collection; in the diffused region, the lifetime is assumed to have been degraded by phosphorus infusion to the extent that recombination far exceeds collection. Therefore,

$$I_D \ll I_B \quad (7)$$

Further, since junction depths for silicon solar cells are not generally greater than 10^{-4} centimeter, for short wavelength radiation,

$$e^{-\alpha X_j} \cong e^{-(10^4)(10^{-4})} = \frac{1}{e} \quad (8)$$

As a consequence of equations (7) and (8), the dependence of short wavelength response on junction depth can be approximated as

$$I_{\alpha} = I_B e^{-\alpha X_j} \quad (9)$$

Diffusion

If the diffusion conditions achieve a saturated concentration of phosphorus at the silicon surface, the phosphorus concentration $C(X)$ at a depth X is (ref. 5)

$$C(X) = C(0) \operatorname{erfc} \frac{X}{2\sqrt{Dt}} \quad (10)$$

where D is the diffusion coefficient, t is the time of diffusion, and $C(0)$ is the phosphorus concentration at the surface. This profile is presented in figure 1 along with a

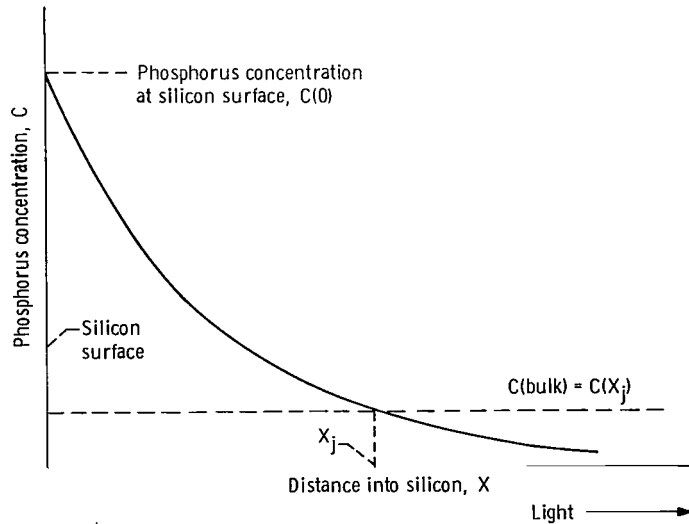


Figure 1. - Phosphorus diffusion profile.

compensating uniform concentration, $C(\text{bulk})$, of p-type dopant. At room temperature, the majority type of dopant atoms can be considered completely ionized except near the point of exact compensation. Here, both types of charge carriers have such low concentrations that a junction may be defined where

$$C(X) = C(\text{bulk}) = C(X_j)$$

The sheet conductance σ_s of the diffused layer is the integral of the electrical conductivity from the surface to the junction:

$$\sigma_s = \int_0^{X_j} q(\mu_n N_n + \mu_p N_p) dX \quad (11)$$

where

q unit electric charge of a carrier

μ_n mobility of electrons

N_n concentration of electrons

μ_p mobility of holes

N_p concentration of holes

For 10-ohm-centimeter p-type silicon, $C(\text{bulk}) \leq 10^{15}$ atoms per cubic centimeter (ref. 6). For diffusion temperatures of 800°C and above, the average n-layer phosphorus concentration is in excess of 5×10^{19} atoms per cubic centimeter (ref. 7). Under these conditions, the compensating effect of the p-type dopant is not significant over most of the diffused layer. Therefore,

$$N_n \approx C(X) \gg N_p \quad (12)$$

The region near the junction where this relation breaks down contributes insignificantly to the integral of equation (11). It is further noted that $\mu_n > \mu_p$ throughout this region (ref. 6). Therefore,

$$\mu_n N_n = \mu_n C(X) \gg \mu_p N_p \quad (13)$$

and equation (11) can be written in good approximation as

$$\sigma_s = \int_0^{X_j} q \mu_n C(X) dX \quad (14)$$

Since μ_n is constant for concentrations above 6×10^{19} atoms per cubic centimeter (ref. 8), equation (14) can be further simplified to

$$\sigma_s = q \mu_n \int_0^{X_j} C(X) dX \quad (15)$$

When equations (10) and (15) are combined,

$$\sigma_s = q \mu_n \int_0^{X_j} C(0) \operatorname{erfc}\left(\frac{X}{2 \sqrt{Dt}}\right) dX \quad (16)$$

With the substitution

$$\xi = \frac{X}{2 \sqrt{Dt}}$$

equation (16) becomes

$$\sigma_s = q \mu_n C(0) 2 \sqrt{Dt} \int_0^{X_j/2 \sqrt{Dt}} \operatorname{erfc}(\xi) d\xi \quad (17)$$

This integral is a function only of $X_j/2 \sqrt{Dt}$. In order to show that this, in turn, is only a function of diffusion temperature, write equation (10) for $X = X_j$ as

$$\operatorname{erfc}\left(\frac{X_j}{2 \sqrt{Dt}}\right) = \frac{C(X_j)}{C(0)} \quad (18)$$

where $C(X_j)$ is a constant and depends only on $C(\text{bulk})$. However, $C(0)$, the surface saturation concentration, depends on the temperature of the diffusion. Since

$$\operatorname{erfc} \frac{X_j}{2\sqrt{Dt}} = \text{function of temperature} \quad (19)$$

its argument, $X_j/2\sqrt{Dt}$, is also a function only of temperature. Equation (17) reduces to

$$\sigma_s = A(T)\sqrt{t} \quad (20)$$

From the foregoing, it is also seen that

$$\sqrt{t} = (\text{function of } T)X_j \quad (21)$$

Equation (20) can alternatively be written as

$$\sigma_s = A'(T)X_j \quad (22)$$

Relation of Spectral Response to Diffusion Conditions

Equation (9) indicates that the blue response of silicon solar cells is dependent on the depth of the diffused junction. Equation (22) indicates that the sheet conductance of the diffused layer is proportional to the junction depth. A combination of these two equations gives the relation between blue response and sheet conductance as

$$I_\alpha = I_B e^{-[\alpha/A'(T)]\sigma_s} \quad (23)$$

At a constant diffusion temperature, $\log I_\alpha$ will be a linear function of sheet conductance and will increase as the sheet conductance decreases. Deviations from equation (23) can be expected at the limit of very shallow junctions as evidenced by low sheet conductance where surface effects, high internal resistance, and poor junction formation become important. In particular, poor junction formation can result in high reverse leakage. The leakage effect is expected to be a random phenomenon, but the probability of a serious leakage path existing between the bulk region and the n-layer contacts on any given cell would be greater with shallower junction depths. Therefore, in terms of a production process for fabricating extremely shallow-junction cells, one would expect to obtain lower yields of acceptable solar cells.

EXPERIMENT

The dependence of the solar cell performance on diffusion temperature is expected to be affected by the solubility and diffusivity of phosphorus in silicon. The diffusivity is by far the stronger function of temperature (refs. 6, 8, and 9). The diffusion coefficient always enters the equations multiplying the diffusion time. For this reason, time and temperature effects were studied in the same experiments. Diffusion temperatures of 800° to 1000° C were employed, 800° C being approximately the threshold of effective diffusion of phosphorus in silicon. Examining the properties of extremely shallow junctions necessitated employing a range of diffusion times that extended to the shortest possible intervals, which, in the present experiment, were 1 minute.

The sources employed included P_2O_5 , $POCl_3$, and elemental phosphorus. The compound P_2O_5 is widely used in this type of work. Because of its ease in handling, $POCl_3$ has recently gained wider use in solar cell fabrication work. Elemental phosphorus was included to provide a comparison of oxidized phosphorus to unoxidized phosphorus as a source material.

The three carrier gases, oxygen, nitrogen, and forming gas, were used and served as an oxidizing, an inert, and a reducing atmosphere, respectively. Forming gas is a mixture of 6 percent hydrogen and 94 percent nitrogen.

In the present investigation, all the solar cells were fabricated from boron-doped silicon single crystals grown at the NASA Lewis Research Center by the crucible method. Only 10-ohm-centimeter silicon crystals were used. These crystals were cut into wafers 1 by 2 centimeters. Prior to diffusion, the wafers were treated in a three-step process: (1) the surfaces were degreased in a series of organic solvents; (2) they were etched in a solution of acetic, nitric, and hydrofluoric acids which produced a polished surface; and (3) they were subjected to a series of rinses in hot (not boiling) distilled and deionized water. All chemicals employed were transistor grade.

The diffusions were performed in a fused quartz tube heated by a two-temperature zone furnace. Silicon wafers were introduced into the heated tube on a slotted fused quartz boat and were mounted vertically by means of a clean glass suction grip. The carrier gas was passed through a liquid-nitrogen cold trap and into the diffusion tube at a rate of 4 liters per minute. The wafers were introduced at the discharge end of the tube while the phosphorus source and carrier gas were introduced into the inlet end. Diffusion temperatures were measured with a Chromel-Alumel thermocouple placed in a sealed quartz tube attached to the diffusion boat and were held constant to within $\pm 2^\circ$ C during the diffusion.

Of the three types of phosphorus sources used, only the P_2O_5 powder employed the second temperature zone available in the furnace. In this case, a fused quartz boat con-

taining P_2O_5 was placed in a $280^\circ C$ region of the furnace. At this temperature, it sublimed and was carried to the wafer surfaces by the carrier gas.

In the case of the $POCl_3$ liquid, the carrier gas bubbled through the source. A system of stopcocks provided a source bypass without opening the system.

Elemental phosphorus was obtained by the reduction of phosphorus trichloride (PCl_3) in forming gas. The gas bubbled through the PCl_3 and into the diffusion furnace. During the reduction, red phosphorus powder deposited onto the cold portion of the quartz tube. When this region was subsequently heated, the phosphorus sublimed and was carried to the wafer surfaces.

The measurement of diffusion time was the most precise when $POCl_3$ was employed. The system of stopcocks allowed startup times reproducible to within 2 seconds. The compound P_2O_5 and elemental phosphorus diffusions were timed from the instant the source was exposed to its heating medium. No quantitative temperature data are available for elemental phosphorus. Sublimation of the red phosphorus was visually observed to begin at about 15 seconds after heat was applied to the tube. Source boat temperature, in the case of P_2O_5 , was monitored with a thermocouple. The temperature was observed to reach $270^\circ C$ at the end of the first minute. A temperature of $280^\circ C$ was attained between 4 and 5 minutes from startup. This means, of course, that P_2O_5 diffusions for times less than 4 minutes never attained $280^\circ C$. It has been found, however, that a source temperature of $250^\circ C$ is sufficiently high to attain saturation of phosphorus on the silicon surface.

Source behavior was visually monitored in terms of white fumes at the exhaust end of the furnace. These fumes were observed for all three sources. With $POCl_3$, these fumes always began between 22 and 24 seconds after startup. For P_2O_5 and elemental phosphorus, they were first observed between 30 and 45 seconds after startup. All diffusions were considered terminated when the wafers were withdrawn from the furnace while the sources were still active.

Postdiffusion processing involved applying silver cerium contacts by a method developed at Lewis. The n-layer contact geometry shown in figure 2 is required for cells with a high blue response and a low sheet conductance.

All the electrical measurements were performed on completed solar cells except the measurement of sheet conductance. A four-point probe method (ref. 10) was used to measure the sheet resistance on one wafer from each diffusion. Sheet conductances reported are the reciprocal of this and have units of squares per ohm. The junction leakage was determined by measuring with an oscilloscope the dark current produced when the cell was under 0.6 volt reverse bias. The blue response was measured in terms of the short-circuit current generated by light from the 0.4-micrometer-wavelength filter of the Lewis filter wheel solar simulator (ref. 11). The calibration of

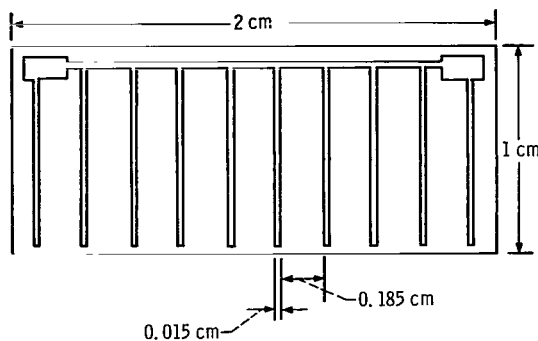


Figure 2. - Contact geometry of n-layer employed in present investigation.

this instrument permits calculation of outer space current produced by a 0.05-micrometer bandwidth centered at 0.4 micrometer.

Current-voltage curves of the illuminated cells were made under a tungsten light source by using an X, Y-plotter. The fill factor was calculated, as a percentage, from these data as follows:

$$\text{Fill factor} = \frac{(\text{maximum power})(100)}{(\text{short-circuit current})(\text{open-circuit voltage})} \frac{\text{mW}}{(\text{mA})(\text{V})}$$

No attempt was made to duplicate the exact outer space solar spectrum for this measurement. Instead, the illumination level was set to produce approximate outer space short-circuit current from a standard silicon solar cell. This procedure is found at this laboratory to give fill factor values equal to those obtained under the solar spectrum.

RESULTS AND DISCUSSION

Time and Temperature Study

For these experiments, P_2O_5 and POCl_3 were employed as the phosphorus sources, and oxygen was used as the carrier gas. Data from this study are plotted in figures 3 to 7. For clarity, these graphs are restricted to the data for 800° , 900° , and 950° C diffusions. Data have been obtained for 840° , 875° , 925° , and 1000° C and follow the same trends.

In figure 3, the log of short-circuit current generated by the light passing the 0.4-micrometer solar simulator filter is plotted against the sheet conductance of the cell. This curve is in accordance with equation (23), which predicts a linear relation where the slope = $-\alpha/A'(T)$; A' and possibly the absorption coefficient α for

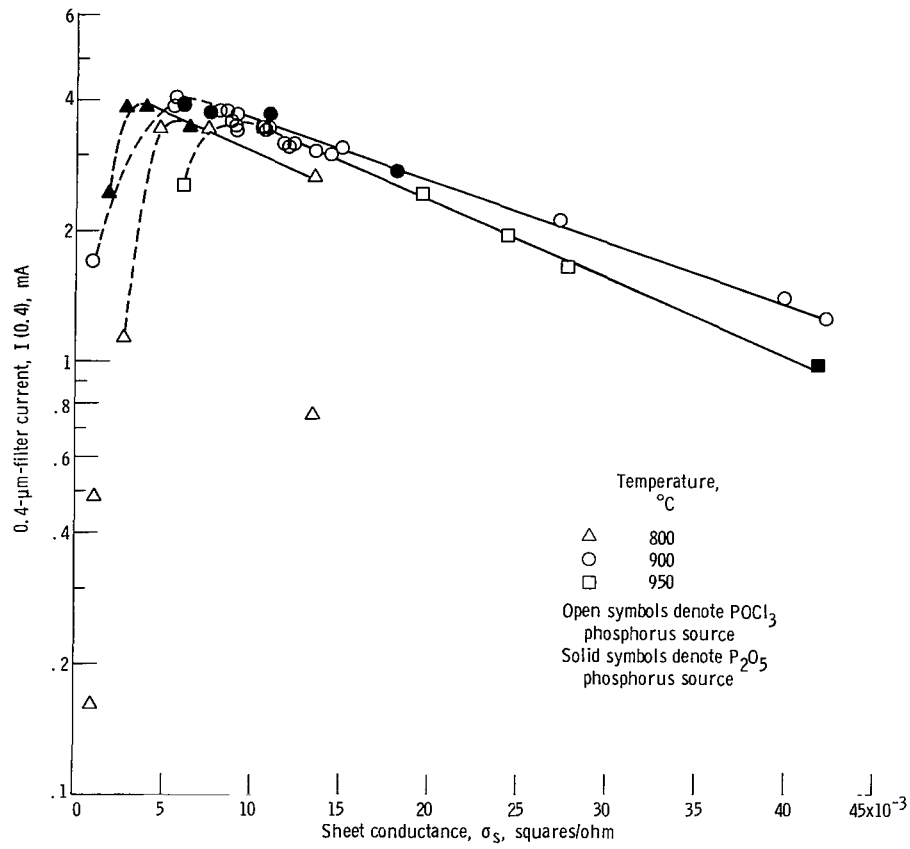


Figure 3. - 0.4-Micrometer-filter current as function of sheet conductance.

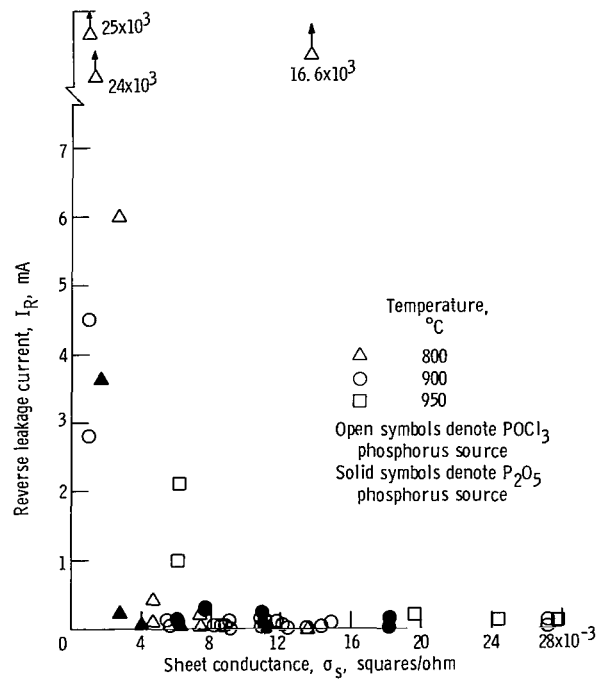


Figure 4. - Reverse leakage current as function of sheet conductance. All diffusions in oxygen.

0.4-micrometer light in silicon are functions of the diffusion temperature because of their dependence on average n-layer phosphorus concentration. The data show good agreement with this functional relation over most of the range of conductance values. Over this range, the highest blue response at a given sheet conductance is achieved at a diffusion temperature near 900°C .

Below conductance values near 5×10^{-3} square per ohm, the blue response drops rapidly. Figure 4 show that this drop in response coincides with a rapid rise in reverse leakage current of the junction. There was little difference in the peak blue response achieved for all the temperatures, but the peak occurred at a lower conductance at a lower temperature. At 800°C , the peak response was lower for the POCl_3 than for the P_2O_5 .

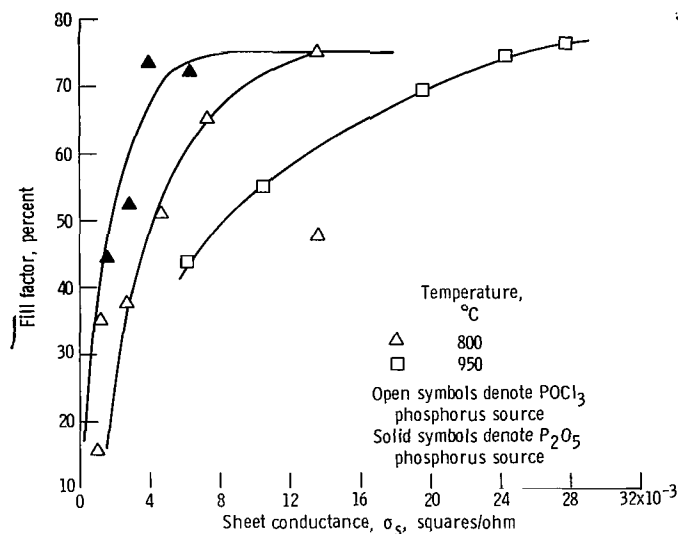


Figure 5. - Fill factor as function of sheet conductance. All diffusions in oxygen.

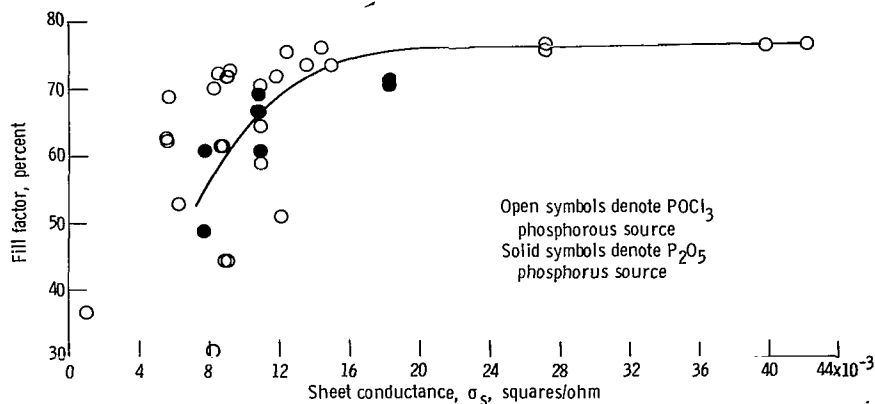


Figure 6. - Fill factor as function of sheet conduction at 900°C . All diffusions in oxygen.

In figures 5 and 6, the fill factor data are presented as a function of sheet conductance. The curves drawn through the data are reproduced for comparison in figure 7. At all temperatures, the fill factor decreases for low values of sheet conductance. In addition, the temperature dependence of these data is much more evident than for the blue response data of figure 3. The fill factor degradation for diffusion temperatures of 800° and 900° C appears to coincide with the onset of high reverse leakage, as observed in the blue response data. However, it does not appear possible to attribute the 950° C fill factor degradation entirely to high reverse leakage. It can be seen in figure 5 that

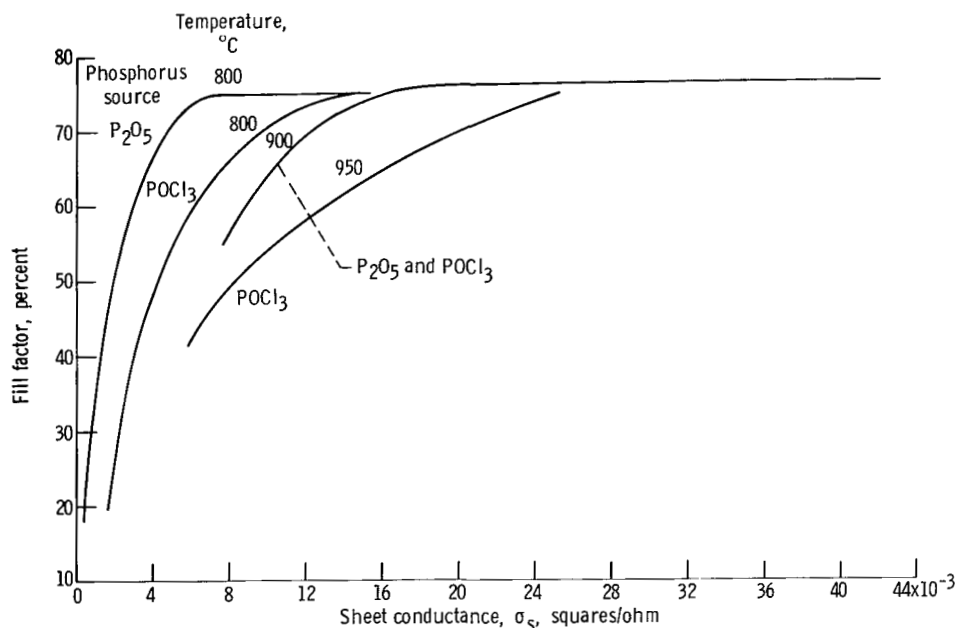


Figure 7. - Comparison of curves of fill factor as function of sheet conductance at 800°, 900°, and 950° C. Diffusions in oxygen.

significant fill factor degradation occurs for sheet conductance values greater than 10×10^{-3} square per ohm, whereas in figure 4 no significant reverse leakage occurs for sheet conductance above 7×10^{-3} square per ohm. For all temperatures, the fill factor reaches a maximum value of 75 percent at high sheet conductance values.

It may be concluded from these data that, when high blue response is desired to improve stability to radiation, the sheet conductance values should not exceed 10×10^{-3} square per ohm. The lower limit on useful sheet conductance is set by the onset of high reverse leakage and fill factor degradation. Since fill factor degradation (for cells with a sheet conductance of 10×10^{-3} square/ohm or less) is markedly greater at temperatures above 900° C, diffusion temperatures should be kept below 900° C.

Comparison of Phosphorus Sources

The data presented in figures 3 to 6 provide comparison of P_2O_5 and $POCl_3$ at all temperatures in the presence of oxygen. No significant difference is observed between the two sources for diffusion temperatures greater than $800^\circ C$. At $800^\circ C$, however, the blue response and fill factor of cells fabricated with $POCl_3$ seem generally lower than those of cells fabricated with P_2O_5 .

In figures 8 and 9 the quantity σ_s^2 is plotted as a function of the measured diffusion time. The data agree with equation (20) if the diffusion times are first corrected for an induction period t_0

$$\sigma_s = A(T) \sqrt{t_m - t_0} \quad (24)$$

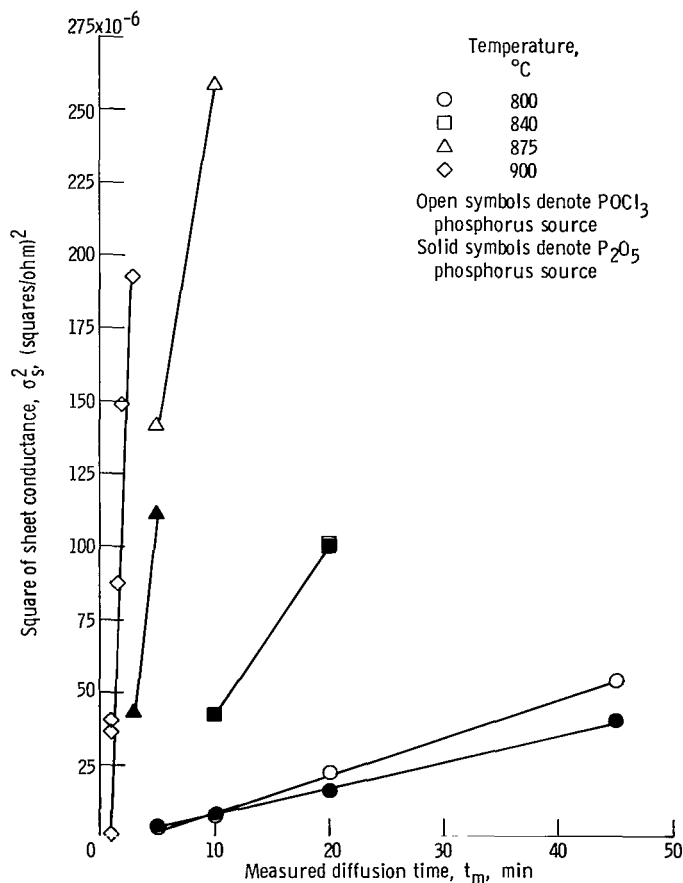


Figure 8. - Square of sheet conductance as function of measured diffusion time. All diffusions in oxygen.

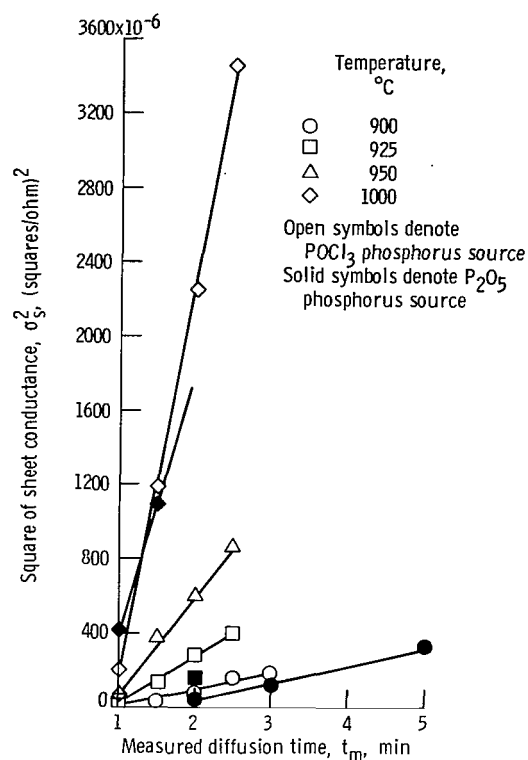


Figure 9. - Square of sheet conductance as function of diffusion time. All diffusions in oxygen.

where t_m is the measured diffusion time and t_o appears to be a decreasing function of temperature.

Data on elemental phosphorus diffused cells are compared with the other two phosphorus sources in table I. In table I(a), sheet conductance data for 20-minute diffusion at 840°C, a standard solar cell fabrication diffusion condition, are compared for all source and carrier gas combinations. The values of sheet conductance reported as less than 1.0×10^{-3} square per ohm represent what are considered unsuccessful diffusions. Not enough phosphorus entered the silicon to ensure conversion to n-type over the entire surface. The elemental phosphorus forming gas combination produces as high a sheet conductance as most of the other successful combinations.

In table I(b), sheet conductance, fill factor, reverse leakage, and blue response for all elemental phosphorus diffusions that produced solar cells are presented. For comparison, diffusions employing P₂O₅ and POCl₃ in oxygen as the carrier gas are also listed. The 840°C, 20-minute condition plus three sets of conditions for producing very low sheet conductance are presented. Within each shallow-junction combination, the elemental phosphorus diffused cells have higher leakage than cells made with the other

TABLE I. - COMPARISON OF ELEMENTAL PHOSPHORUS DIFFUSIONS WITH THOSE OF P_2O_5 AND $POCl_3$ (a) Data for standard cell diffusion
condition of 840°C , 20 minutes

Carrier gas	Phosphorus source		
	P_2O_5	$POCl_3$	Elemental phosphorus
Sheet conductance, σ_s , squares/ohm			
Forming	18.5×10^{-3}	$< 1.0 \times 10^{-3}$	11.9×10^{-3}
Nitrogen	-----	9.6×10^{-3}	$< 1.0 \times 10^{-3}$
Oxygen	10.0×10^{-3}	10.0×10^{-3}	-----

(b) Cell characteristics

Diffusion condition	Phosphorus source and carrier gas											
	P_2O_5 in oxygen				$POCl_3$ oxygen				Elemental phosphorus in forming gas			
	Sheet conductance, σ_s , squares/ohm	Reverse leakage, I_R , μA	Fill factor, percent	0.4- μm filter current, $I(0.4)$, mA	Sheet conductance, σ_s , squares/ohm	Reverse leakage, I_R , μA	Fill factor, percent	0.4- μm filter current, $I(0.4)$, mA	Sheet conductance, σ_s , squares/ohm	Reverse leakage, I_R , μA	Fill factor, percent	0.4- μm filter current, $I(0.4)$, mA
840°C 20 min	10.0×10^{-3}	29	75	3.35	10.0×10^{-3}	42	76	3.43	11.9×10^{-3}	72	--	3.10
										61	--	3.14
										300	--	3.23
875°C 3 min	6.5×10^{-3}	43	60	3.89	-----	----	---	----	14.0×10^{-3}	870	47	2.26
									1.7×10^{-3}	81 000	34	1.04
									0.7×10^{-3}	11 400	31	.86
875°C 5 min	11.0×10^{-3}	14	71	3.54	12.0×10^{-3}	99	75	3.34	0.8×10^{-3}	58 000	36	0.25
									9.6×10^{-3}	760	48	2.30
900°C 1 min	-----	---	---	---	1.0×10^{-3} 6.2×10^{-3}	2800	37	1.65	1.3×10^{-3}	19 800	26	0.56
						1060	36	2.20	-----	-----	---	----
						114	53	3.80	-----	-----	---	----

two sources. It was decided that further elemental phosphorus experiments would not be fruitful because of the nonreproducibility of sheet conductance as a function of diffusion time and temperature.

Comparison of Carrier Gases

In table II, the data for the carrier gases oxygen, nitrogen, and forming gas are presented for P_2O_5 diffusions at 900°C for similar diffusion times. At a given diffusion

TABLE II. - DATA FOR COMPARISON OF CARRIER GASES USING P_2O_5 AS PHOSPHORUS SOURCE

Diffusion temperature, $^\circ\text{C}$	Carrier gas	Measured time, t_m , min	Sheet conductance, σ_s , squares/ohm	Number of cells	Reverse leakage range, I_R , μA	Fill factor ^a	0.4- μm filter current, ^a $I(0.4)$, mA
900	Oxygen	2	6.1×10^{-3}	2	116 to 122	-----	(3.89)3.92, 3.86
		2	7.6	2	184 to 300	(54.5)48.5, 61.1	(3.72)3.60, 3.84
		3	10.9	3	1 to 234	(65.7)60.9, 66.9, 69.2	(3.67)3.77, 3.67, 3.57
		5	18.2	3	34 to 150	(71.0)70.8, 71.1	(2.70)2.68, 2.68, 275
900	Nitrogen	2	13.1×10^{-3}	1	25	74.5	3.25
		3	16.6	1	25	75.7	2.77
		5	19.5	1	3	75.9	2.44
900	Forming	2	14.5×10^{-3}	1	54	74.6	3.10
		3	16.1	↓	6	73.6	2.69
		5	19.5		3	74.6	2.60
		10	24.7		3	75.0	1.94

^aWhere more than one cell is available, average used in fig. 10 or 11 is presented in parentheses.

time, nitrogen and forming gas produce higher sheet conductances than oxygen. When the silicon oxide forms on the wafer surface, the phosphorus trapped in it can no longer contribute to diffused-layer sheet conduction. This leads to a lower effective surface concentration of phosphorus. With oxygen present, the silicon surface is oxidized faster than when the other carrier gases are used.

In figure 10, the 0.4-micrometer filter current is plotted against the sheet conductance for P_2O_5 diffusions at 900°C and with the three carrier gases. No significant differences are observed between these three sets of data as to magnitude of the currents or to the slope of the dependence on σ_s .

In figure 11, the fill factors of these cells are plotted against sheet conductance. The oxygen data show a drop in fill factor at low sheet conductance, as was observed in

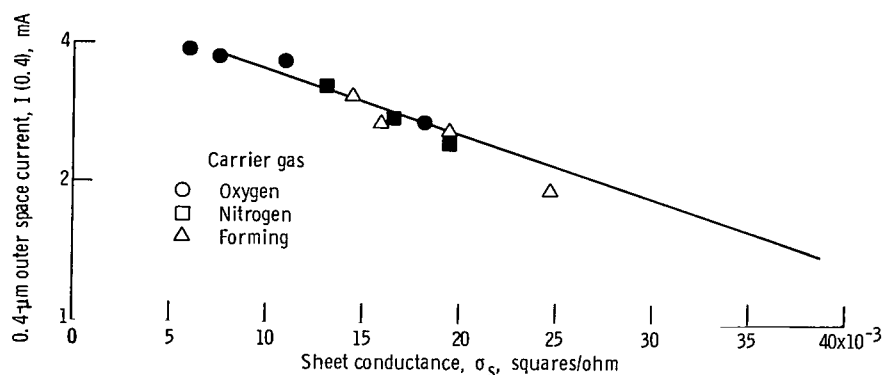


Figure 10. - Blue response as function of sheet conductance for P_2O_5 at 900° C.

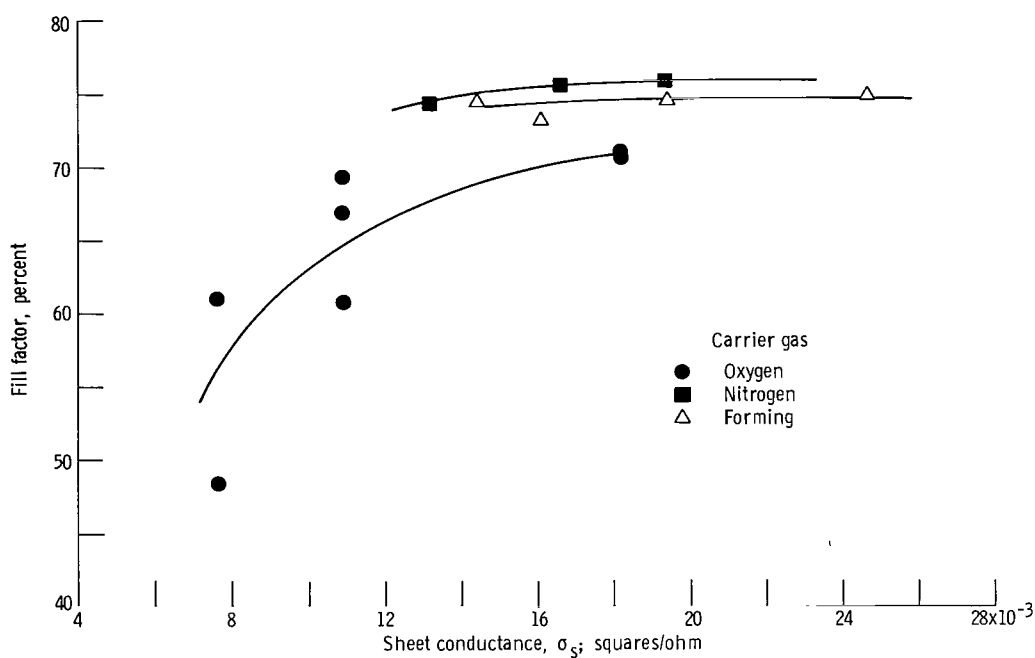


Figure 11. - Fill factor as function of sheet conductance for P_2O_5 at 900° C.

figures 5 to 7. Since it was not practical to use P_2O_5 diffusion for times shorter than 2 minutes, it was not possible to obtain nitrogen or forming gas cells with sheet conductance as low as that with oxygen.

From the limited data, it is not possible to determine whether or not oxygen produces lower fill factors than the other two carrier gases.

SUMMARY OF RESULTS

A study was made of the effects of varying the diffusion time, temperature, phosphorus source, and carrier gas in the fabrication of shallow-junction n-on-p silicon solar cells. The effects were measured in terms of the 0.4-micrometer (blue) response, the fill factor, and the reverse leakage of these cells. The following results were obtained:

1. In the phosphorus diffusion temperature range of 800° to 1000° C, the blue response was related to the junction depth of the diffused n-layer, as measured in terms of sheet conductance.
2. The blue response decreased at sheet conductance values lower than 5×10^{-3} square per ohm.
3. The fill factor decreased as the sheet conductance decreased. The fill factor decreased more slowly at the lower diffusion temperatures. The fill factor approached a limit of about 75 percent for high sheet conductance. Degradation of the fill factor at low sheet conductance appeared to correlate with the onset of high reverse leakage. For diffusion temperatures above 900° C, the fill factor degradation began at a higher sheet conductance.
4. The fill factor had a greater diffusion temperature dependence than did the blue response.
5. When high blue response is important, the sheet conductance should be less than 10×10^{-3} square per ohm. However, the diffusion temperature should be below 900° C to minimize the loss of the fill factor.
6. In applications where radiation stability is not a prime objective, solar cells with sheet conductance above 10×10^{-3} square per ohm (and, therefore, with a low blue response) will result in less sensitivity of fill factor to diffusion conditions and higher yields of low-reverse-leakage solar cells.
7. At 800° C, cells fabricated with phosphorus pentoxide (P_2O_5) had generally higher blue responses and fill factors in the low sheet conductance range than did cells made with phosphorus oxychloride ($POCl_3$). No significant differences were observed for diffusion temperatures above 800° C.
8. No significant difference in blue response or fill factor was observed between cells diffused with P_2O_5 in oxygen, nitrogen, or forming gas to the same value of sheet conductance.
9. For a given diffusion time, forming gas and nitrogen produced higher sheet conductance values than oxygen.

10. Cells made by diffusing elemental phosphorus in forming gas had higher reverse current leakages than cells diffused with P_2O_5 and $POCl_3$ in oxygen when compared for very shallow junctions. In addition, sheet conductance values were less reproducible than those for P_2O_5 and $POCl_3$ diffusions in oxygen.

Lewis Research Center,
National Aeronautics and Space Administration,
Cleveland, Ohio, October 29, 1969,
120-33.

APPENDIX - SYMBOLS

$C(X)$	concentration of phosphorus at distance X from surface of silicon wafer, atoms/cm ³
$C(0)$	concentration of phosphorus at surface of silicon wafer, atoms/cm ³
D	diffusion coefficient of phosphorus in silicon, cm ² /sec
$\text{erfc}(X/2 \sqrt{Dt})$	complimentary error function, $X/2 \sqrt{Dt}$
I_B	current coefficient of bulk region, mA/cm ²
I_D	current coefficient of diffused region, mA/cm ²
I_α	current collected by solar cell due to light of absorption coefficient α , mA/cm ²
N_n	concentration of free electrons
N_p	concentration of free holes
q	electric charge on an electron, C
R	flux of photons at distance X into cell, number/(cm ²)(sec)
R_T	total number of photons absorbed in cell per area and time, number/(cm ²)(sec)
t	diffusion time, sec
X_B	thickness of solar cell, cm
X_j	distance of p-n junction from illuminated surface of solar cell, cm
α	absorption coefficient of light of given wavelength in silicon, cm ⁻¹
μ_n	mobility of electrons in n-type silicon, cm ² /(V)(sec)
μ_p	mobility of holes in n-type silicon, cm ² /(V)(sec)
σ_s	sheet conductance, squares/ohm

REFERENCES

1. Mandelkorn, J.; et al.: Fabrication and Characteristics of Phosphorus-Diffused Solar Cells. J. Electrochem. Soc., vol. 109, no. 4, Apr. 1962, pp. 313-318.
2. Babcock, Richard V.: An Explanation of the Superior Radiation Resistance of p-Type Base Si Solar Cells. J. Electrochem. Soc., vol. 108, no. 12, Dec. 1961, pp. 1119-1122.
3. Mandelkorn, Joseph: New Silicon Solar Cell for Space Use. Proceedings 20th Annual Power Sources Conference. PSC Publ. Committee, May 1966, pp. 194-197.
4. Anon.: Silicon. EPIC Data Sheet, Hughes Aircraft Co., May 1964.
5. Crank, J.: The Mathematics of Diffusion. Clarendon Press, Oxford, 1956, p. 19.
6. Irvin, John C.: Resistivity of Bulk Silicon and of Diffused Layers in Silicon. Bell Syst. Tech. J., vol. 41, no. 2, Mar. 1962, pp. 387-410.
7. Trumbore, F. A.: Solid Solubilities of Impurity Elements in Germanium and Silicon. Bell Syst. Tech. J., vol. 39, no. 1, Jan. 1960, pp. 205-233.
8. Tannenbaum, Eileen: Detailed Analysis of Thin Phosphorus-Diffused Layers in p-Type Silicon. Solid State Electr., vol. 2, no. 1, Mar. 1961, pp. 123-132.
9. Mackintosh, I. M.: The Diffusion of Phosphorus in Silicon. J. Electrochem. Soc., vol. 109, no. 5, May 1962, pp. 392-401.
10. Smits, F. M.: Measurement of Sheet Resistivities with the Four-Point Probe. Bell Syst. Tech. J., vol. 37, no. 3, May 1958, pp. 711-718.
11. Manderlkorn, Joseph; Broder, Jacob D.; and Ulman, Robert P.: Filter-Wheel Solar Simulator. NASA TN D-2562, 1965.

NATIONAL AERONAUTICS AND SPACE ADMINISTRATION
WASHINGTON, D. C. 20546
OFFICIAL BUSINESS

FIRST CLASS MAIL



POSTAGE AND FEES PAID
NATIONAL AERONAUTICS AND
SPACE ADMINISTRATION

02U 001 28 51 3DS 70013 00903
AIR FORCE WEAPONS LABORATORY /WLOL/
KIRTLAND AFB, NEW MEXICO 87117

ATT E. LOU BOWMAN, CHIEF, TECH. LIBRARY

POSTMASTER: If Undeliverable (Section 158
Postal Manual) Do Not Return

"The aeronautical and space activities of the United States shall be conducted so as to contribute . . . to the expansion of human knowledge of phenomena in the atmosphere and space. The Administration shall provide for the widest practicable and appropriate dissemination of information concerning its activities and the results thereof."

— NATIONAL AERONAUTICS AND SPACE ACT OF 1958

NASA SCIENTIFIC AND TECHNICAL PUBLICATIONS

TECHNICAL REPORTS: Scientific and technical information considered important, complete, and a lasting contribution to existing knowledge.

TECHNICAL NOTES: Information less broad in scope but nevertheless of importance as a contribution to existing knowledge.

TECHNICAL MEMORANDUMS: Information receiving limited distribution because of preliminary data, security classification, or other reasons.

CONTRACTOR REPORTS: Scientific and technical information generated under a NASA contract or grant and considered an important contribution to existing knowledge.

TECHNICAL TRANSLATIONS: Information published in a foreign language considered to merit NASA distribution in English.

SPECIAL PUBLICATIONS: Information derived from or of value to NASA activities. Publications include conference proceedings, monographs, data compilations, handbooks, sourcebooks, and special bibliographies.

TECHNOLOGY UTILIZATION PUBLICATIONS: Information on technology used by NASA that may be of particular interest in commercial and other non-aerospace applications. Publications include Tech Briefs, Technology Utilization Reports and Notes, and Technology Surveys.

Details on the availability of these publications may be obtained from:

SCIENTIFIC AND TECHNICAL INFORMATION DIVISION
NATIONAL AERONAUTICS AND SPACE ADMINISTRATION
Washington, D.C. 20546